Figure(s)
Click here to download high resolution image

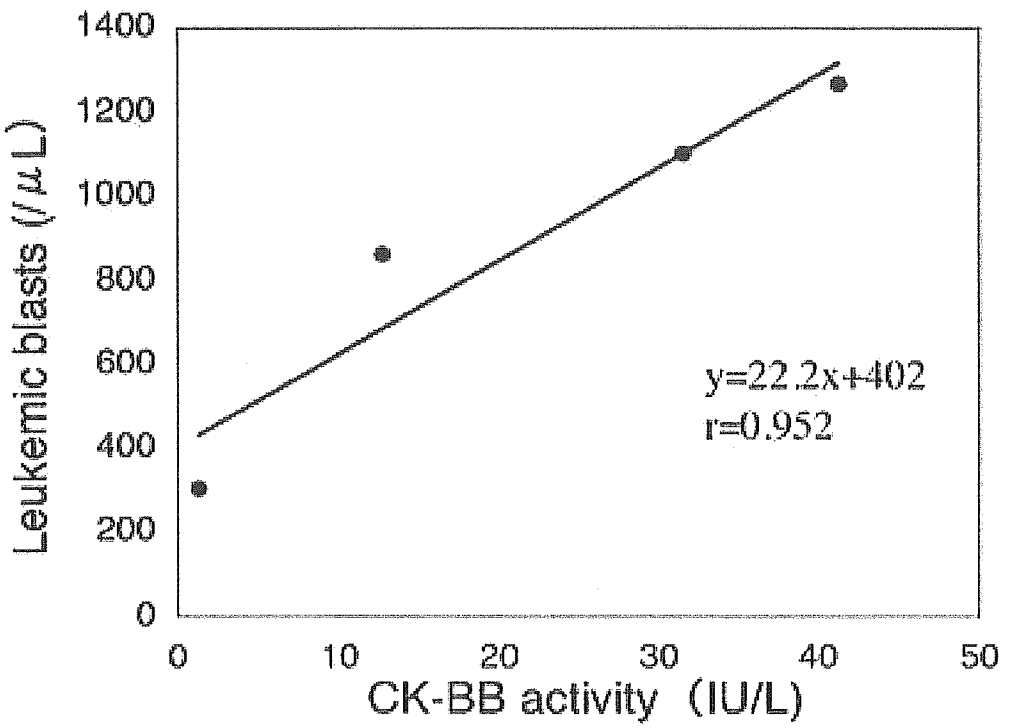

Figure(s)

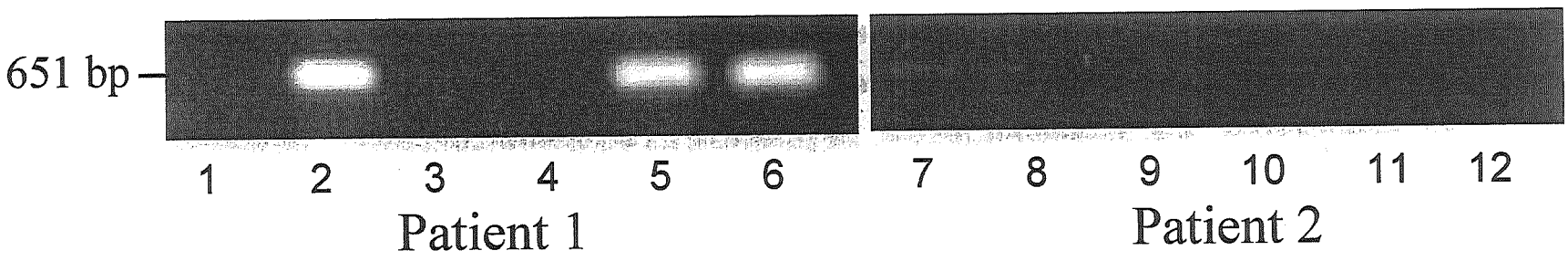

Figure(s)

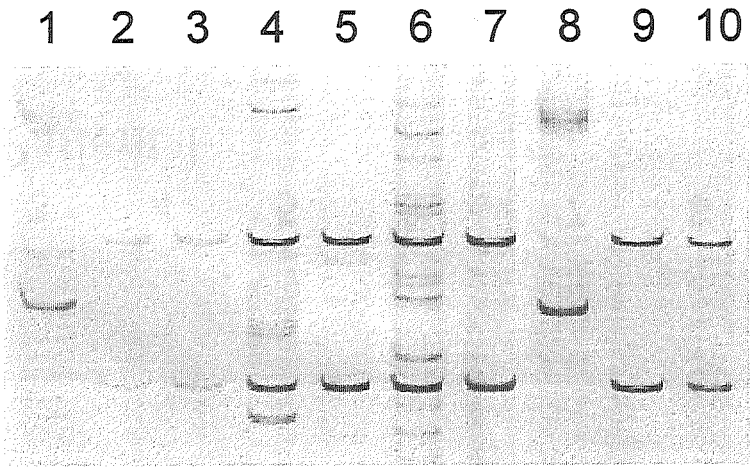

Figure(s)

MKN7

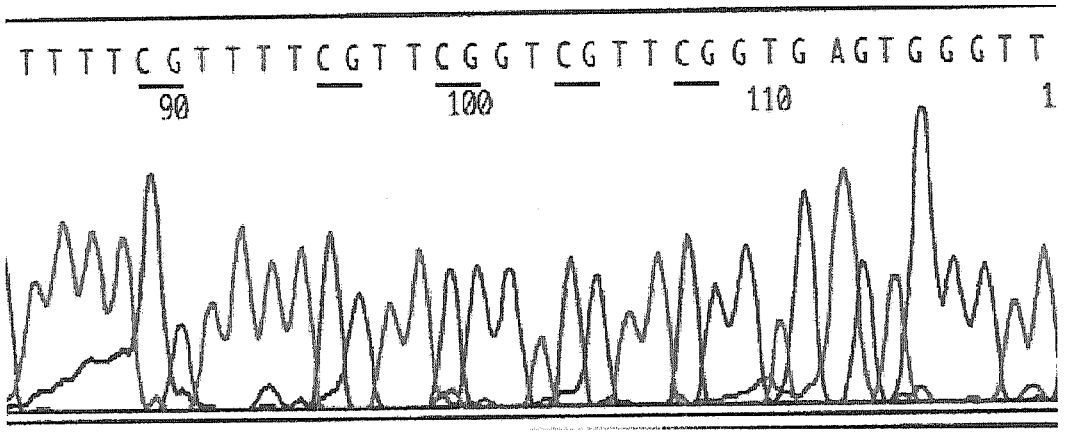

Patient 1

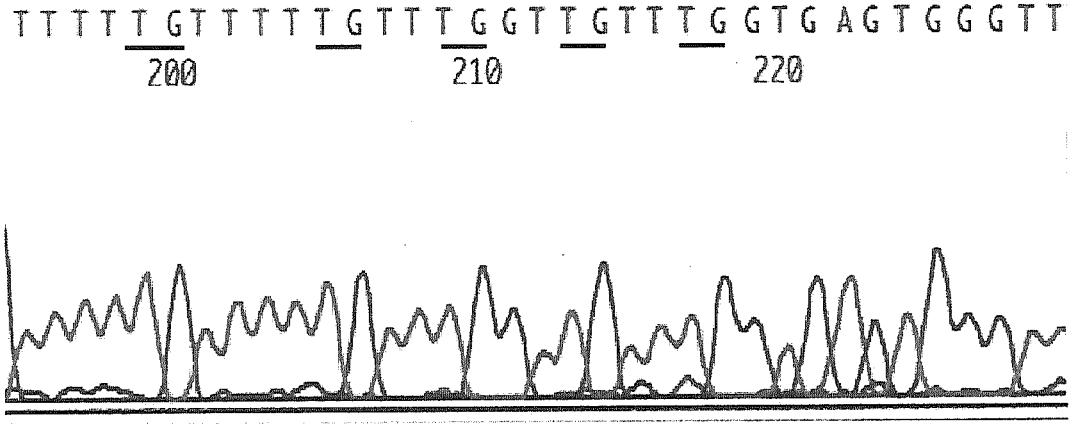

ELSEVIER

Clinica Chimica Acta 355 (2005) 181–184

www.elsevier.com/locate/clinchim

Pilot study of arbitrarily primed PCR-single stranded DNA conformation polymorphism analysis for screening genetic polymorphisms related to specific phenotypes

Masato Maekawa[a,*], Terumi Taniguchi[a], Takeshi Uramoto[a], Hitomi Higashi[a], Toshinobu Horii[a], Akihiro Takeshita[a], Haruhiko Sugimura[b], Masao Kanamori[c]

[a]*Department of Laboratory Medicine, Hamamatsu University School of Medicine, 1-20-1 Handayama, Hamamatsu 431-3192, Japan*
[b]*First Department of Pathology, Hamamatsu University School of Medicine, Hamamatsu, Japan*
[c]*Department of Life Sport, Biwako Seikei Sport College, Shiga, Japan*

Received 16 November 2004; received in revised form 27 December 2004; accepted 27 December 2004

Abstract

Background: To investigate relationships between phenotypes and genotypes is not simple. We propose a phenotype-to-genotype screening strategy and pooled DNA system. As a pilot study of this strategy, we used arbitrarily primed polymerase chain reaction (AP-PCR) in combination with single-stranded DNA conformation polymorphism (SSCP) to screen for genetic polymorphisms associated with longevity.

Methods: Study subjects were separated into 3 age groups, individuals aged >100 years, 90–99 years and 60–69 years. Genomic DNAs were prepared from each individual, pooled to represent the 5 study groups, and then the pooled genomic DNAs were subjected to AP-PCR-SSCP analysis.

Results: We found 1 SNP more frequently in senior citizens with longevity. The genotype frequency of the 82133G>A polymorphism of human chromosome 3 clone RP11-61K12 (AC011199) differed significantly (P=0.0189, Fisher's exact test) between older subjects (>90 years) and younger subjects (<70 years). It is noteworthy that the strategy we describe herein was useful for identifying an SNP that showed statistically significant differences in its distribution across the subject groups.

Conclusions: The pooled DNA strategy and quantitative genotype discrimination can also be applied to screening for the relationship between phenotype and genotype more effectively.

Keywords: Arbitrarily primed PCR; Genetic polymorphism; Phenotype; Single stranded DNA conformation polymorphism

* Corresponding author. Tel.: +81 53 435 2721; fax: +81 53 435 2794.
E-mail address: mmaekawa@hama-med.ac.jp (M. Maekawa).

0009-8981/$ - see front matter © 2005 Elsevier B.V. All rights reserved.
doi:10.1016/j.cccn.2004.12.004

1. Introduction

Associations between phenotypes and single nucleotide polymorphisms (SNPs) or other polymorphisms, including insertions and deletions, have been shown by exhaustive screening of polymorphisms by sequencing and by etiological studies of genotype–phenotype correlations. This genotype-to-phenotype approach is useful; however, exhaustive screening is expensive and labor intensive. Relationships between phenotypes and genotypes have also been investigated by use of candidate genes for the phenotype. However, much effort cannot always lead to a good result [1]. Here we propose the reverse process, a phenotype-to-genotype screening strategy and pooled DNA system. In essence, we screened for common genotypes in pooled DNAs of individuals with a common phenotype. As a pilot study of this strategy, we used arbitrarily primed polymerase chain reaction (AP-PCR) [2] in combination with single-stranded DNA conformation polymorphism (SSCP). This technique takes advantage of the random nature of AP-PCR and the quantitative and resolution abilities of SSCP [3,4]. We used this method to screen for genetic polymorphisms associated with longevity.

2. Materials and methods

2.1. Subjects

Study subjects were separated into 3 groups, individuals aged >100 years (n=9), 90–99 years (3 sub-groups, n=8 each group), and 60–69 years (n=9). As a control group, we included 27 volunteers <30 years recruited from among medical students.

2.2. AP-PCR-SSCP

Genomic DNAs were prepared from each individual and then pooled to represent the 3 age groups described above. The pooled genomic DNAs were subjected to AP-PCR-SSCP analysis. Sequences of the primers used are shown in Table 1. Amplification conditions for AP-PCR were 94 °C for 3 min followed by 5 cycles of 94 °C for 1 min, 42 °C for 1 min, and 72 °C for 2 min, 35 cycles at 94 °C for 0.5 min, 55 °C for 0.5 min, and 72 °C for 1 min, and a final cycle of 72 °C for 7 min. The amplified products were analyzed by SSCP with 6–10% polyacrylamide gel electrophoresis and silver staining detection (Daiichi Pure Chemicals, Tokyo, Japan) [4]. SSCP bands with different visual densities or mobilities were excised from the gel and cloned into pGEM-T (Qiagen, Tokyo, Japan) for sequencing (PE Applied Biosystems, Tokyo, Japan). Nucleotide sequences were searched with BLAST [5]. Gene-specific primers were synthesized and used for genotyping of individual genomic DNAs in 3 age groups and a control group of volunteers by PCR-SSCP and/or DNA sequencing.

Table 1
Primer sequences for the present study

Primer name	Primer sequence (5′ to 3′)
LDAcDF1	ACCGCCCGACGTGCATTCCC
LDAcDF2	CGCCCGACGTGCATTCCCGA
LDHA-m3	GTAATTATCATGGCTGGGACAT
Ae6F	TGAGGTGATCAAACTCAAAGGC
Ae6R	CTTAATCATGGTGGAAACTGGG
BAT26F	TGACTACTTTTGACTTCAGCC
BAT26R	AACCATTCAACATTTTTAACCC
MS3(A)F2	CCAGCTATCTTCTGTGCATC
UF1KABI	CGAATCGCATGGCCTTG
EU1KABI	TTCTCAGGCTCCCTCTCC
p16RNA1	CCCGCTTTCGTAGTTTTCAT
p16RNA2	TTATTTGAGCTTTGGTTCTG
D16S521L	GGAGCGAGACTCCGTCTAAA
D9S287L	GAGGATGCTCCTCACGC
NCC-COMM	AGGAATTCTTTTCTCTTNCAG

2.3. Statistical analysis

Pearson's χ^2 test and Fisher's exact test were used to compare allele and genotype frequencies between study groups. To analyze allele frequencies between the four age categories, the Kruskal–Wallis non-parametric test was used. Statistical significance was accepted at $P<0.05$.

3. Results and discussion

From a polyacrylamide gel of AP-PCR-SSCP (Fig. 1), we found 1 suspected band with different densities. By nucleotide sequence, it was originated from the 82133G>A polymorphism of human

chromosome 3 clone RP11-61K12 (AC011199). We synthesized gene-specific primers and genotyped each individuals by PCR-SSCP analysis. The genotype frequency of the 82133G>A polymorphism of human chromosome 3 clone RP11-61K12 (AC011199) differed significantly (P= 0.0189, Fisher's exact test) between older subjects (>90 years) and younger subjects (<70 years) (Table 2). Differences in allele and genotype frequencies between the four age categories were not statistically significant.

The SNP was located in a mammalian-wide interspersed repeat (MIR) on chromosome 3 and was described in GeneBank. MIRs are one of the most common interspersed repeats in primates, with an estimated 300,000 copies per genome that account for 1–2% of the total DNA [6]. It is not clear whether this SNP is associated with longevity; however, it is noteworthy that the strategy we describe herein was useful for identifying an SNP that showed statistically significant differences in its distribution across the subject groups.

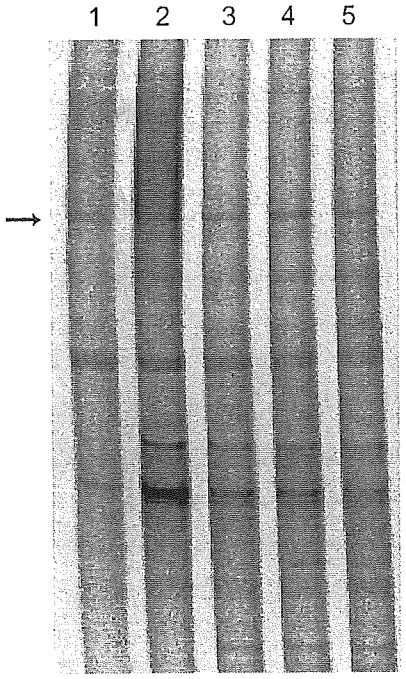

Fig. 1. Electropherogram of AP-PCR-SSCP. The AP-PCR product amplified by using Ae6R primer was separated by SSCP analysis (6% polyacrylamide gel electrophoresis at 15 °C for 5 h). A stained band with different mobility and density (shown as arrow; observed as slightly broad band in lane 1) was excised from the gel, cloned, and sequenced. As a result of sequential examinations, an SNP of the human chromosome 3 clone was found. Lane 1, individuals aged more than 100 years (n=9); lanes 2–4, individuals aged 90–99 years (3 sub-groups, n=8 each group); lane 5, individuals aged 60–69 years (n=9).

Table 2
Genotype and allele frequencies of the 82133G>A polymorphism on human chromosome 3 clone RP11-61K12 (AC011199) in subjects classified by age

Age	Genotype			G allele		A allele	
	G/G	G/A	A/A	No.	%	No.	%
≥100 years	4	5	0	13	72	5	28
90–99 years	10	11	0	31	74	11	26
60–69 years	1	6	2	8	44	10	56
<30 years	9	13	5	31	57	23	43
>90 years	13*	16*	0*	44	73	16	27
<70 years	10*	19*	7*	39	54	33	46

* The genotype frequency differed significantly (P=0.0189, Fisher's exact test) between older subjects (>90 years) and younger subjects (<70 years).

In the present pilot study, we used mini-gel, for SSCP. If large gels with long separations or 2-dimensional separation with detection by fluorescence dyes are used, better resolution could be obtained. Both the phenotype-to-genotype screening strategy and semi-quantitative distribution measurement using pooled DNA may be useful in screening for important genetic variations associated with a variety of human diseases and phenotypes. The advanced improvement of precise techniques is clearly necessary, however, the pooled DNA strategy and quantitative genotype discrimination can also indicate the relative proportion of different genotypes, haplotypes or allelotypes at glance and be applied to screening for the relationship between phenotype and genotype more effectively.

Acknowledgements

This research was supported in part by Health and Labor Sciences Research Grants for Third Term Comprehensive Control Research for Cancer (H15-9 and H16-018), by Grants-in-Aid for Exploratory Research (15659133) from the Japan Society for the Promotion of Science, and by the Nakatani Electronic Measuring Technology Association of Japan.

References

[1] Um J-Y, Lee K-M, Kim H-M. Polymorphism of interleukin-1 receptor antagonist gene and obesity. Clin Chim Acta 2004; 340:173–7.

[2] Welsh J, McClelland M. Fingerprinting genomes using PCR with arbitrary primers. Nucleic Acids Res 1990;18:7213–8.

[3] Peinado MA, Malkhosyan S, Velazquez A, Perucho M. Isolation and characterization of allelic losses and gains in colorectal tumors by arbitrarily primed polymerase chain reaction. Proc Natl Acad Sci U S A 1992;89:10065–9.

[4] Maekawa M, Sugano K, Ushiama M, Masuda T, Ohkura H, Kakizoe T, et al. Relative ratios of mRNA molecules encoded by genes with homologous sequences using fluorescence-based single-strand conformation polymorphism analysis. Biochem Biophys Res Commun 1996;223:520–5.

[5] National Center for Biotechnology Information. BLAST. http://www.ncbi.nlm.nih.gov/BLAST/.

[6] Smit AF, Riggs AD. MIRs are classic, tRNA-derived SINEs that amplified before the mammalian radiation. Nucleic Acids Res 1995;23:98–102.

Glycobiology vol. 15 no. 9 pp. 887–894, 2005
doi:10.1093/glycob/cwi071
Advance Access publication on May 4, 2005

Polysialic acid facilitates tumor invasion by glioma cells

Masami Suzuki[1,3,4], Misa Suzuki[1,4], Jun Nakayama[1,5], Atsushi Suzuki[3,4], Kiyohiko Angata[4], Shihao Chen[4], Keiichi Sakai[6], Kazuki Hagihara[7], Yu Yamaguchi[7], and Minoru Fukuda[2,4]

[4]Glycobiology, Cancer Research Center, The Burnham Institute, La Jolla, CA 92037; [5]Department of Pathology, Shinshu University School of Medicine, Matsumoto 390-8621, Japan; [6]Department of Neurosurgery, Shinshu University School of Medicine, Matsumoto 390-8621, Japan; [7]Developmental Neurobiology Programs, Cancer Research Center, The Burnham Institute, La Jolla, CA 92037

Received on March 15, 2005; revised on April 26, 2005; accepted on April 27, 2005

Polysialic acid (PSA) is thought to attenuate neural cell adhesion molecule (NCAM) adhesion, thereby facilitating neural cell migration and regeneration. Although the expression of PSA has been shown to correlate with the progression of certain tumors such as small cell lung carcinoma, there have been no studies to determine the roles of PSA in gliomas, the most common type of primary brain tumor in humans. In this study, we first revealed that among patients with glioma, PSA was detected more frequently in diffuse astrocytoma cells, which spread extensively. To determine directly the role of PSA in glioma cell invasion, we transfected C6 glioma cells with polysialyltransferases to express PSA. In those transfected cells, PSA is attached mainly to NCAM-140, whereas the mock-transfected C6 cells express equivalent amounts of PSA-free NCAM-140. Both PSA negative and positive C6 cell lines exhibited almost identical growth rates measured in vitro. However, PSA positive C6 cells exhibited increased invasion to the corpus callosum, where the mock-transfected C6 glioma cells rarely invaded when inoculated into the brain. By contrast, the invasion to the corpus callosum by both the mock-transfected and PSA positive C6 cells was observed in NCAM-deficient mice. These results combined indicate that PSA facilitates tumor invasion of glioma in the brain, and that NCAM–NCAM interaction is likely attenuated in the PSA-mediated tumor invasion.

Key words: polysialic acid/glioma/tumor invasion/NCAM/polysialyltransferases

Introduction

Polysialic acid (PSA) is a unique carbohydrate of a linear homopolymer of α2,8-linked sialic acid (Finne, 1982). PSA is primarily attached to *N*-glycans of the neural cell adhesion molecule (NCAM) in neural cells (Finne, 1982; Edelman, 1984; Rutishauser and Landmesser, 1996; Kiss and Rougon, 1997; Kleene and Schachner, 2004), whereas it is attached to mucin-type glycoproteins in human breast carcinoma and leukemic cells (Martersteck *et al.*, 1996). Polysialylated NCAM is abundant in the embryonic brain. Most NCAM in the adult brain does not contain PSA, but polysialylated NCAM is continuously present in the hippocampus and olfactory bulbs, where neuronal generation persists in the adult (Edelman, 1984; Rutishauser and Landmesser, 1996; Kiss and Rougon, 1997; Kleene and Schachner, 2004).

The cDNAs-encoding polysialyltransferases have been cloned, and these enzymes are called ST8Sia IV (also called PST) and ST8Sia II (also called STX) (Livingston and Paulson, 1993; Eckhardt *et al.*, 1995; Nakayama *et al.*, 1995; Scheidegger *et al.*, 1995; Yoshida *et al.*, 1995). Both ST8Sia II and ST8Sia IV catalyze the transfer of multiple α2,8-linked sialic acid residues to a glycan containing NeuNAcα2→3/6Galβ1→4GlcNAc→R (Angata *et al.*, 2000). During development, the expression of *ST8Sia II* and *ST8Sia IV* genes is specifically regulated (Hildebrandt *et al.*, 1998a; Ong *et al.*, 1998). The amount of ST8Sia II is more significantly reduced postnatally compared with ST8Sia IV (Hildebrandt *et al.*, 1998a; Ong *et al.*, 1998). Mutant mice with ST8Sia II deficiency exhibited misguidance of infrapyramidal mossy fibers and the formation of ectopic synapses in the hippocampus. This altered hippocampus development was associated with higher exploratory drive (Angata *et al.*, 2004). Mutant mice with ST8Sia IV deficiency, on the other hand, bore a restricted phenotype involving an impairment of long-term potentiation in the hippocampal CA1 region (Eckhardt *et al.*, 2000). These results suggest that ST8Sia II and ST8Sia IV may differentially direct the synthesis of PSA in temporal and spatial-specific manners.

PSA has been found in various tumors including small cell and nonsmall cell lung carcinomas, multiple myeloma, neuroblastoma, and Wilms' tumor (Roth *et al.*, 1988; Van Camp *et al.*, 1990; Fukuda, 1996; Smith *et al.*, 1996; Hildebrandt *et al.*, 1998b; Seidenfaden *et al.*, 2000; Tanaka *et al.*, 2000). In both small cell and nonsmall cell lung carcinomas and multiple myeloma, the expression of PSA is correlated with tumor progression (Scheidegger *et al.*, 1994; Smith *et al.*, 1996; Hildebrandt *et al.*, 1998b; Tanaka *et al.*, 2000). In one particular study, small cell lung carcinoma cells expressing different amounts of PSA were isolated from H69 cell line by clonal dilution of cells. After subcutaneous inoculation of these tumor cells, tumor cells expressing PSA produced

[1]These authors contributed equally to this work.
[2]To whom correspondence should be addressed; e-mail: minoru@burnham.org
[3]Present address: Department of Obstetrics and Gynecology, Keio University School of Medicine, Tokyo 160-8582, Japan

more intracutaneous metastasis than tumor cells poorly expressing PSA, although a comparable amount of NCAM was expressed in these variants (Scheidegger *et al.*, 1994).

Gliomas are the most common type of primary brain tumors in humans. It is highly invasive in nature, but tumor metastasis to other organs is rare (Thorsen and Tysnes, 1997). To elucidate the mechanisms of glioma invasion and migration, transfections of various genes to glioma cell lines have been tested for tumor invasion and migration (Kaye *et al.*, 1986; Edvardsen *et al.*, 1994; Chicoine and Silbergeld, 1995; Thorsen and Tysnes, 1997; Owens *et al.*, 1998). In particular, the forced expression of NCAM-140 in glioma cell lines resulted in reduced migration when the glioma cells were inoculated into the brain (Edvardsen *et al.*, 1994) or assayed for migration through a reconstituted basal lamina, Matrigel (Chicoine and Silbergeld, 1995). However, no studies have addressed the direct roles of PSA in glioma invasion in the brain.

In this study, we first found that among the 44 patients with astrocytoma examined, PSA was detected in nine cases of the 30 NCAM-positive astrocytoma, in particular, a diffuse astrocytoma subtype which spreads extensively. ST8Sia IV and ST8Sia II transcripts were also detected in a recurred case of diffuse astrocytoma, which expressed PSA. We then assayed experimental tumor formation of C6 rat glioma cell line in the brain after transfection with ST8Sia II or ST8Sia IV cDNA to express PSA. Mock-transfected and PSA-positive C6 cell lines were inoculated into the brain of wild type and NCAM-deficient mice. The results obtained indicate that PSA expressed on glioma cells facilitates tumor invasion, most likely due to the attenuation of NCAM–NCAM interaction.

Results

Expression of PSA, ST8Sia II mRNA, and ST8Sia IV mRNA in human astrocytoma

Immunohistochemistry by using anti-NCAM monoclonal antibody demonstrated that NCAM was expressed along cytoplasmic processes of the tumor cells in 30 (68.2%) of 44 patients examined, irrespective of the histological grade of the tumor, that is, five cases (83.3%) of six pilocytic astrocytoma, 10 (66.7%) of 15 diffuse astrocytoma, 11 (68.8%) of 16 anaplastic astrocytoma, and four (57.1%) of seven glioblastoma multiforme. On the other hand, PSA was immunohistochemically detected in nine (30%) of 30 patients, which also expressed NCAM in the tumor cells; one case (20%) of pilocytic astrocytoma, four cases (40%) of diffuse astrocytoma, three cases (27.3%) of anaplastic astrocytoma, and one case (25%) of glioblastoma multiforme (Figure 1). Clinical records of the patients at the surgical operation revealed that four (44.4%) of nine PSA-positive patients were recurred cases, whereas five (23.8%) of 21 patients expressing NCAM alone were recurred cases. This result suggests that PSA expressed on the tumor cells was associated with recurrence of the disease. These results combined with the morphological examination of tumor cells suggest that PSA is expressed more frequently in those gliomas that spread extensively, which makes it difficult to remove all of the glioma cells in the first operation.

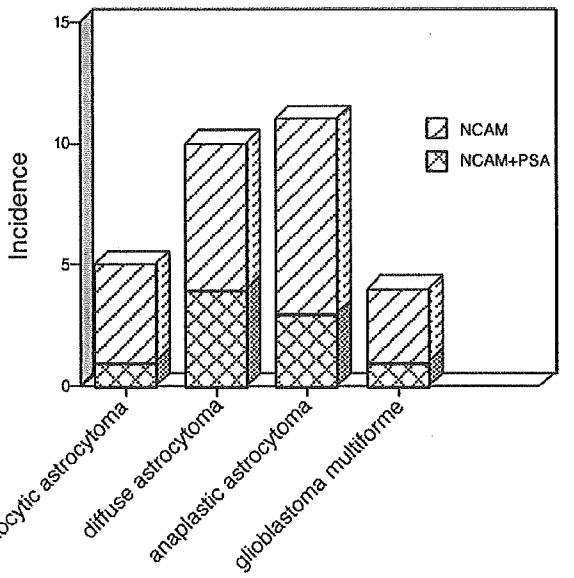

Fig. 1. Expression of polysialic acid (PSA) and neural cell adhesion molecule (NCAM) in human astrocytomas. Expression of NCAM and PSA was examined by using 123C3 anti-NCAM antibody and 5A5 anti-PSA antibody. Among NCAM-positive tumor cells, the numbers of PSA-positive tumor cells are also shown.

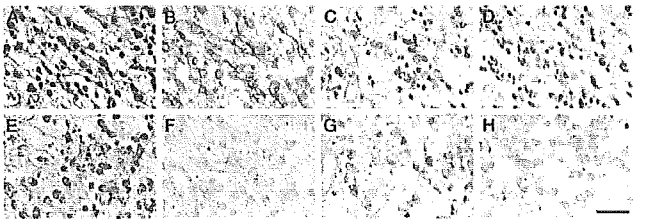

Fig. 2. Expression of polysialic acid (PSA) and ST8Sia II and ST8Sia IV transcripts in a recurred case of diffuse astrocytoma invading contralateral cerebral hemisphere through corpus callosum. The tumor stained with hematoxylin and eosin shows a protoplasmic astrocytoma proliferating in a loose microcystic matrix (**A**). In parallel sections, neural cell adhesion molecule (NCAM) was detected by 123C3 antibody (**B**), and PSA was stained by 5A5 antibody before (**C**) and after (**D**) endo-neuraminidase-*N* (endo-*N*) treatment. Parallel sections were also subjected to in situ hybridization by using antisense probes for ST8Sia IV (**E**) and ST8Sia II (**G**) and sense probes for ST8Sia IV (**F**) and ST8Sia II (**H**). All the photographs are shown in the same magnification (bar = 50 μm).

Indeed in one recurred case of diffuse astrocytoma, significant amounts of PSA (Figure 2C) as well as NCAM (Figure 2B) were detected in the cell surface and cytoplasmic processes of tumor cells, and the magnetic resonance imaging of this patient revealed that the recurred tumor mainly occupied the right frontal lobe of cerebrum and invaded the left frontal lobe through the corpus callosum. To determine whether two polysialyltransferases, ST8Sia II and ST8Sia IV, play a major role in the biosynthesis of PSA in the glioma cells, we analyzed serial tissue sections of the above case by in situ hybridization using specific RNA probes for ST8Sia II and ST8Sia IV. The results show that both ST8Sia II (Figure 2G) and ST8Sia IV (Figure 2E)

transcripts were detectable in the tumor cells, and ST8SiaIV apparently plays a major role in the polysialylation of this tumor.

Isolation of C6 glioma cells expressing PSA

To directly demonstrate the roles of PSA in glioma invasion, we measured tumor formation of C6 glioma cells after the cells were transfected with ST8Sia II or ST8Sia IV cDNA. After transfecting with pcDNA3-ST8Sia II or pcDNA3-ST8Sia IV, clonal cell lines expressing PSA were isolated, resulting in C6-ST8Sia II and C6-ST8Sia IV. As shown in Figure 3A, C6-ST8Sia II and C6-ST8Sia IV were positive for both PSA and NCAM, whereas the mock-transfected C6 cell line was positive only for NCAM. The results also demonstrated that all three cell lines express almost identical amounts of NCAM as assessed by fluorescence activated cell sorter (FACS) analysis.

Western blot analysis of C6, C6-ST8Sia II, and C6-ST8Sia IV illustrates that PSA-containing proteins migrated as a large heterogeneous molecular mass of 170–240 kDa (Figure 3B). After removing PSA by endoneuraminidase-*N* (endo-*N*) digestion, NCAM molecules migrated at almost the same position as the NCAM of C6 cells and NCAM-140 expressed on HeLa cells. The results also show that a small amount of NCAM-180 is expressed although this band might also represent a dimer of NCAM-140 (Angata *et al.*, 1997). These results indicate that most PSA is attached to NCAM-140 in C6-ST8Sia II and C6-ST8Sia IV. NCAM was estimated to contain 20–40 sialic acids and 10–35 sialic acids for C6-ST8Sia II and C6-ST8Sia IV cells, respectively, using the procedure described previously (Angata *et al.*, 1998). Polysialylation by ST8Sia IV was less efficient than that by ST8Sia II, probably because C6 cells that express a large amount of PSA after transfection by ST8Sia IV tend to detach from the substratum.

Expression of PSA does not increase cell growth

To determine whether the expression of PSA facilitates tumor cell growth in vitro, the cells were plated at low density and the growth rate was determined. The results demonstrated that the expression of PSA did not alter the rate of tumor cell growth when assessed by a cell proliferation assay in vitro (Figure 4).

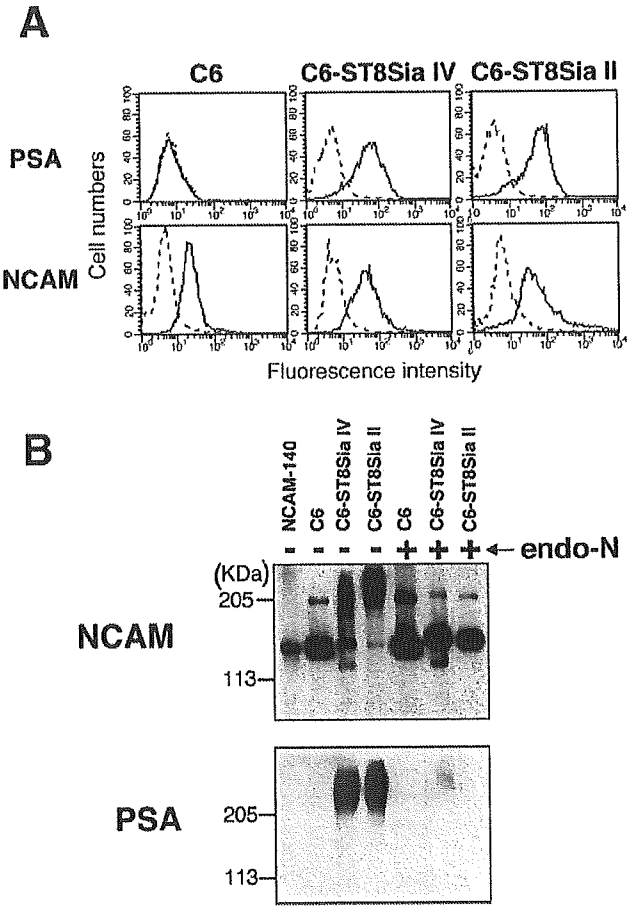

Fig. 3. Expression of neural cell adhesion molecule (NCAM) and polysialic acid (PSA) in C6 cells and C6 cells transfected with ST8Sia IV or ST8Sia II cDNA. **(A)** The cells were stained with 12F8 anti-PSA antibody or 5B8 anti-NCAM antibody followed by fluoroscein isothiocyanate-conjugated secondary antibody (anti-rat IgM for PSA and anti-mouse IgG for NCAM) and subjected to flow cytometric analysis. Dotted lines indicate a control omitting the primary antibodies. **(B)** The cells shown in panel A were subjected to western blot analysis before (–) and after (+) endoneuraminidase-*N* (endo-*N*) treatment. NCAM and PSA were detected with the same antibodies used in panel A. HeLa cells expressing NCAM-140 (NCAM-140) were treated in the same manner.

Tumor invasion of C6 glioma cells expressing PSA

Although many of invasion studies were carried out in vitro using for example, Matrigel, this assay is not suited for studying invasion in the brain because substantial differences exists in the extracellular components between Matrigel and the brain (Yamaguchi, 2000). We thus opted to utilize in vivo invasion assay.

When the mock-transfected C6 glioma cells were inoculated into the caudate putamen, tumor cells gradually spread to surrounding tissue and then mostly to the cerebral cortex (Figure 5A and B), consistent with C6 glioma derived from diffuse fibrillary astrocytoma (Thorsen and Tysnes, 1997). When PSA-expressing C6-ST8Sia II cells were inoculated in the same manner, more tumor invasion was observed, in particular, to the corpus callosum (Figure 5D–F). These tumor cells were positive for PSA, and the positive staining was abolished by pretreatment with endo-*N* (Figure 5G and H). It is noteworthy that each glioma cell highly extended along myelinated fibers in the corpus callosum (Figure 5E insert), in contrast to spindle shape of the mock-transfected C6 cells (Figure 5B insert). Similar results were obtained for PSA-expressing C6-ST8Sia IV cells (Figure 6). By contrast, C6 cells negative for PSA scarcely exhibited invasion to the corpus callosum under the same conditions (Figures 5B and C and 7). Almost identical results were obtained on more than two independently cloned cells.

Invasion to corpus callosum in the absence of NCAM

The above results showed that the invasion of PSA-expressing C6 cells to the corpus callosum may be one of the important

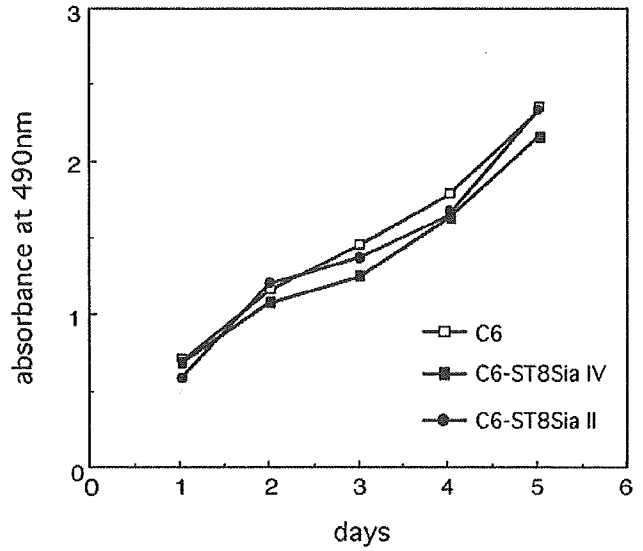

Fig. 4. Comparison of C6 glioma cell growth in vitro. In vitro growth kinetics of the mock-transfected C6, C6-ST8Sia IV, and C6-ST8Sia II cells are shown.

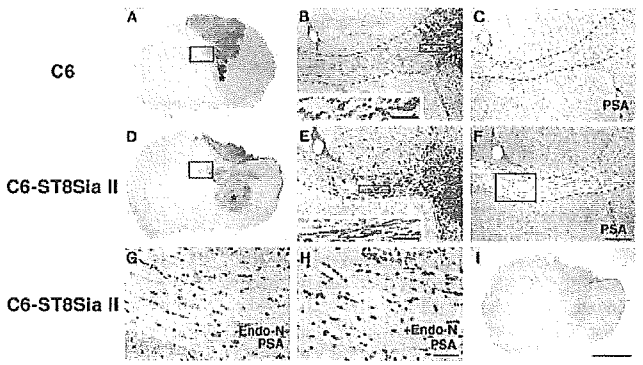

Fig. 5. Invasion of the inoculated C6 glioma cells expressing polysialic acid (PSA) to the corpus callosum of the mice brain. The mock-transfected C6 glioma (**A–C**) and C6-ST8Sia II (**D–I**) cells were injected into the caudate putamen of the brain. Twenty-one days after inoculation, coronal sections of the brain were stained by anti-vimentin antibody (**A, B, D, E**) and anti-PSA antibody, 5A5 (**C, F, G, H**). Digestion with endoneuraminidase-*N* (endo-*N*) was performed before the immunostaining with 5A5 antibody (**H**). Panels **A, D,** and **I** are in the same magnification (bar = 2 mM). Panels **B** and **E** are enlarged figures shown in the box of panels **A** and **D**, respectively, whereas panels **C** and **F** were stained for PSA that are parallel sections of panels **B** and **E** (bar = 200 μm). Inserts in panels **B** and **E** are enlarged figures shown in the box of panels **B** and **E**, respectively (bar = 50 μm). Panels **G** and **H** are enlarged figures shown in the box of panel **F** (bar = 50 μm). Panel **I** indicates a negative control omitting the primary antibodies from the procedure, and no specific staining was found. Envision$^+$ (DAKO) was used for secondary antibody. Counterstaining was performed by hematoxylin. The corpus callosum region and the injected site are shown by dotted lines and a star, respectively.

characteristics in glioma progression. This observation is similar to the fact that axons of the corpus callosum express detectable amounts of PSA on NCAM extending in myelin sheath (Seki and Arai, 1991). To determine whether invasion

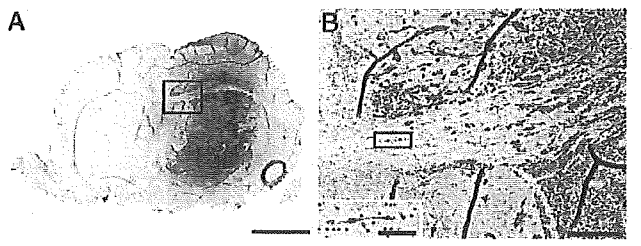

Fig. 6. Invasion to the corpus callosum by C6-ST8Sia IV cells. The invasion assay was carried out in the same way as described in Figure 5. The insert in panel **B** is the enlarged figure indicated in the box of panel **B**, showing extended C6 glioma cells. Bar = 2 mM in panel **A**, 200 μm in panel **B**, and 50 μm in panel **B** insert.

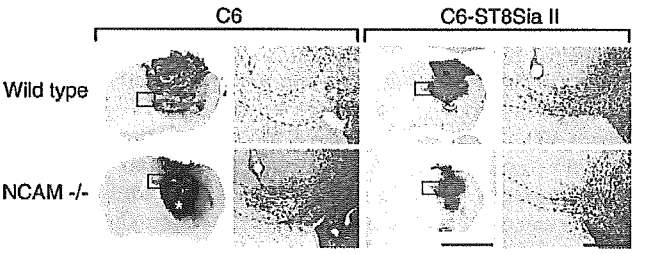

Fig. 7. Invasion of the inoculated C6 glioma cells in the brain of wild type and neural cell adhesion molecule (NCAM)-deficient mice. The mock-transfected C6 glioma and C6-ST8Sia II cells were inoculated into the brain of wild type and NCAM-deficient (NCAM-/-) mice, and the brain was examined in the same way as shown in Figure 5. Right panel (bar = 200 μm) of each set is the enlarged picture of the box in left panel (bar = 2 mm). Immunodetection of vimentin was carried out by using Ventana ES automated DAB immunohistochemical system (Ventana Medical Systems).

by C6 cells is attenuated by PSA-free NCAM–NCAM interaction, we inoculated C6 and C6-ST8Sia II cells into the brain of NCAM-deficient mice. Figure 7 shows that both C6 and C6-ST8Sia II cells invaded into the corpus callosum in NCAM-deficient mice. The results indicate that NCAM–NCAM interaction may prevent C6 cells from invading the corpus callosum in wild-type mice brain, and C6 cells lacking PSA can also invade into the corpus callosum in the absence of NCAM in the host animal.

Discussion

This study demonstrated that glioma cells from patients with astrocytoma express PSA. The frequency of PSA expression was highest in diffuse astrocytoma, which spread extensively, and was apparently associated with recurrence of the disease. We have also revealed that in a patient with recurred diffuse astrocytoma associated with the invasion of corpus callosum, both ST8Sia IV and ST8Sia II confer the expression of PSA on the tumor cells. In previous studies, the overexpression of ST8Sia II has been correlated to the progression of nonsmall cell lung carcinoma (Tanaka *et al.*, 2000). This study expanded these findings to glioma, showing that PSA formed mainly by

ST8Sia IV is associated with the invasive character of glioma cells.

This study also provides direct evidence, for the first time, that PSA plays a role in tumor invasion in the brain. Because glioma tumors rarely metastasize extracranially, we assayed tumor formation inside the brain. C6 glioma cells became highly invasive to the corpus callosum by the acquisition of PSA through the transfection of ST8Sia II or ST8Sia IV. The results strongly suggest that polysialylation facilitates tumor migration. PSA in the transfected C6 glioma cells was shown to attach mostly to the 140-kDa transmembrane NCAM isoform (NCAM-140). Similarly, NCAM-140, but not NCAM-120, is polysialylated in differentiated C2C12 cells (Suzuki *et al.*, 2003). It has been shown that the loss of NCAM-induced metastatic dissemination of pancreatic β cell tumors was observed when β cell tumor-bearing transgenic mice was crossbred with NCAM knockout mice (Perl *et al.*, 1999). This phenotype was reversed by introducing wild-type NCAM-120. These results indicate that PSA attached to NCAM-140 facilitates cell migration. NCAM-140 contains a transmembrane domain, which is absent in NCAM-120. It is tempting to speculate that enhancing glioma invasion may require signal transduction transmitted directly from the extracellular to cytoplasmic domains of NCAM-140. By using TE671 cells that express significant amount of PSA, it has been shown that intraperitoneal injection of TE671 produced lung and liver metastasis. Repeated injection of endo-*N* to remove PSA resulted in the diminishment of lung or liver metastasis (Daniel *et al.*, 2001). Moreover, when metastases occurred in endo-*N*-injected animals, they strongly expressed polysialylated NCAM, which escaped from endo-*N* treatment. These results combined with the results obtained in this study indicate that the expression of PSA leads to increased migration, resulting in increased metastasis.

C6 glioma cells represent a well-differentiated astrocytoma (Thorsen and Tysnes, 1997). After inoculation to the caudate putamen, C6 glioma cells migrated toward the cerebrum cortex and formed tumors in the caudate putamen and cerebrum. Interestingly, PSA-expressing C6 cells invaded the corpus callosum as found in a recurred patient of diffuse astrocytoma. By contrast, such invasion to the corpus callosum was rarely found in the PSA-negative C6 cells. Similarly, PSA expression was more frequently associated with diffuse astrocytoma in the patients examined, suggesting PSA might facilitate cell migration of astrocytoma. The corpus callosum consists of myelinated fibers crossing two hemispheres of the brain. This study also suggests that polysialylated NCAM may weakly interact with adhesive molecules in the corpus callosum (Seki and Arai, 1991), thus allowing cells to migrate in the corpus callosum as shown in previous studies for other systems (Ono *et al.*, 1994; Chazal *et al.*, 2000).

These results, as a whole, indicate that NCAM–NCAM interaction may prevent C6 cells that do not express PSA from migrating into the corpus callosum. It is likely that polysialylation attenuates NCAM–NCAM interaction and facilitates the invasion of polysialylated C6 cells into the corpus callosum. It has also been reported that NCAM may facilitate axonal growth by the stimulation of fibroblast growth factor receptor (Saffell *et al.*, 1997). Similarly, polysialylated NCAM stimulates the signaling by brain-derived neutrophil factor (BDNF), most likely because polysialylated NCAM accumulates BDNF, and presents it to its receptor (Muller *et al.*, 2000; Vutskits *et al.*, 2001; Zhang *et al.*, 2004). Further studies will be necessary to determine if any of those mechanism play a role in glioma invasion facilitated by PSA.

Materials and methods

Tissue collection

Tissue blocks of the primary astrocytomas resected from 44 patients were retrieved from the archives of Shinshu University Hospital, Matsumoto, Japan. According to the World Health Organization (WHO) classification of astrocytic tumors (Kleihuses and Cavenee, 2000), they were categorized into four subtypes, that is, pilocytic astrocytoma (six cases), diffuse astrocytoma (15 cases), anaplastic astrocytoma (16 cases), and glioblastoma multiforme (seven cases). These tissue specimens were fixed for 48 h in 20% buffered formalin (pH 7.4), embedded in paraffin, and sectioned at 4 and 7 μm thickness for immunohistochemistry and in situ hybridization, respectively, as described previously (Machida *et al.*, 2001). The Ethical Committee of Shinshu University School of Medicine approved the protocols for this study.

Immunohistochemistry and in situ hybridization

Immunohistochemical detection of PSA and NCAM was performed by using mouse monoclonal antibodies, 5A5 (mouse IgM, University of Iowa Hybridoma Bank, Iowa City, IA) and 123C3 (mouse IgG_1, Zymed, Carlsbad, CA), respectively. For the NCAM immunostaining, microwave irradiation in a 1.0 mM ethylenediamine tetra-acetic acid (EDTA)–NaOH solution (pH 8.0) was carried out before the incubation with 123C3 antibody, as described previously (Kim *et al.*, 2002). For secondary antibody, Envision$^+$ (DAKO, Glostrup, Denmark), which is dextran polymers conjugating a large number of goat antibodies against mouse immunoglobulins and horseradish peroxidase, was used to increase the sensitivity of immunodetection (Sabattini *et al.*, 1998). The counterstaining was performed with hematoxylin. In control experiments, the primary antibodies were omitted from the staining procedure, and for the PSA staining, pretreatment with endo-*N* that cleaves PSA (Hallenbeck *et al.*, 1987) was also carried out. In these controls, no specific staining was noted.

To construct RNA probes for in situ hybridization, we amplified the ST8Sia IV-specific region (nucleotides −47 to +113; the first nucleotide of the initiation codon is +1) by polymerase chain reaction (PCR) using a primer set of 5′-GCTCTAGAAGGTGCGGGAGCTGG-3′ and 5′-GGGGTACCGATGAGTTGCGTCTCCT-3′. Similarly, the STX-specific region (nucleotides +1 to +138) was amplified by using primers 5′-GCTCTAGATGCAGCTGCAGTTCCGGA-3′ and 5′-GGGGTACCGTTCACAGCTGATCTGATTGT-3′. In these primers, the XbaI and Asp718 sites are underlined. These cDNAs were cloned into the XbaI and Asp718 sites of pGEM-3Zf (+) (Promega, Madison, WI), and the resultant vectors were used as a template for the

construction of the RNA probes, as described previously (Angata *et al.*, 1997; Yeh *et al.*, 2001).

Transfection of C6 glioma cell line with ST8Sia II or ST8Sia IV cDNA vector

pcDNAI-ST8Sia II and pcDNAI-ST8Sia IV harboring cDNA encoding a full-length human ST8Sia II and ST8Sia IV were cloned, as described previously (Nakayama *et al.*, 1995; Angata *et al.*, 1997). The cDNA inserts of pcDNAI-ST8Sia II and pcDNAI-ST8Sia IV were excised by HindIII–XhoI and HindIII–XbaI, respectively, and cloned into corresponding sites of pcDNA3 (Invitrogen, Carlsbad, CA) resulting in pcDNA3-ST8Sia II and pcDNA3-ST8Sia IV.

A rat C6 glioma cell line was transfected with pcDNA3-ST8Sia II or pcDNA3-ST8Sia IV and selected by G418. Clonal cells expressing PSA were chosen after staining with 12F8 anti-PSA antibody (BD Biosciences, San Diego, CA), as described previously (Angata *et al.*, 1997). These cells were designated as C6-ST8Sia II and C6-ST8Sia IV. C6 cells were also transfected with pcDNA3 that lacks cDNA insert, and a cell line isolated after selection with G418 was named mock-transfected C6 cells, C6. These cells were subjected to FACS analysis, as described before (Ohyama *et al.*, 1999).

Western blot analysis

C6, C6-ST8Sia II, and C6-ST8Sia IV cells were subjected to western blot analysis, as described previously (Angata *et al.*, 1997). A portion of cell pellet was digested with endo-*N*. The proteins were separated by sodium dodecyl sulfate–polyacrylamide gel electrophoresis (SDS–PAGE) (6%) and subjected to western blotting using anti-PSA (12F8) or anti-NCAM (5B8) antibody followed by peroxidase-conjugated goat IgG specific to rat IgM or mouse IgG and ECL Plus kit (Amersham Biotech, Piscatany, NJ). HeLa cells expressing NCAM-140 (Nakayama *et al.*, 1995) were used as a positive control.

Cell proliferation assay

C6, C6-ST8Sia II, and C6-ST8Sia IV were seeded in 96-well plates at 10^5 cells/mL in α-MEM Earle's Salts (Irvine Scientific, Santa Ana, CA) containing 10% fetal bovine serum and cultured for various periods. The number of living cells was measured each day by using CellTiter 96® AQueous One Solution Cell Proliferation Assay (Promega), as described previously (Ohyama *et al.*, 1999).

Implantation of C6 cells in mice brain

C6 tumor cells were inoculated into the caudate putamen of adult C57Bl/6 mice, as described previously (Kaye *et al.*, 1986; Chicoine and Silbergeld, 1995). After anesthetizing with tribromoethanol (0.015 mL/g body weight by intraperitoneal injection), C57Bl/6 mice (7- to 9-week-old males, 8 mice for each group of experiments) were set on a stereotaxis frame, and a 1 cm incision was made in the left frontal region of the head. A craniotomy was performed by using a 2-mm bit on a dental drill, and the dura was punctured with a 25-gauge needle. C6 glioma cell suspension [4.8×10^4 cells in 4 μL phosphate-buffered saline (PBS)] was injected by using a Hamilton syringe with a cone-tipped needle attached to the stereotactic frame. Injection was made into the left caudate putamen of the animal at 0.7 mm anterior to the bregma, at 1.8 mm lateral to the midline, and at a depth of 3.0 mm into the brain.

After surgery, the animals were allowed to recover under observation and then returned to their cage. Twenty-one days after surgery, the animals were sacrificed, and brain specimens were prepared for histological analysis. Under the same conditions, C6 and C6-ST8Sia II were inoculated into the brain of mutant mice deficient in NCAM (Cremer *et al.*, 1994) obtained from the Jackson Laboratory (Bar Harbor, ME). NCAM-deficient mice were backcrossed with C57BL/6 mice three generations before use.

Examination of the brain tissue from mice

The mice were deeply anesthetized with tribromoethanol, followed by perfusion with PBS, pH 7.3, and then with 50 mL of 4% paraformaldehyde, 0.2% glutaraldehyde, and 1 mM $MgCl_2$ in 0.1 M sodium phosphate buffer (pH 7.3). Each mouse brain was postfixed in 2% paraformaldehyde, 0.2% glutaraldehyde, and 1 mM $MgCl_2$ in 0.1 M sodium phosphate buffer (pH 7.3) at 4°C overnight. Fixed specimens were embedded in paraffin and cut at 4 μm thickness. Because our preliminary experiments revealed that an intermediate filament, vimentin, which could be detected in astrocytoma (Cosgrove *et al.*, 1989), was strongly expressed in C6 glioma cells (data not shown), the mouse tissue sections were stained with each of two mouse monoclonal antibodies, 5A5 for PSA and V9 mouse IgG_1 (DAKO) for vimentin, followed by treatment with Envision$^+$ (DAKO), as described above, or Ventana ES automated DAB immunohistochemical system (Ventana Medical Systems, Tucson, AZ) (Hayama *et al.*, 2002). The V9 antibody was developed by immunizing swine vimentin and cross-reacts with human, rat, and chicken vimentins. For vimentin staining, microwave irradiation for 25 min in 0.05 M Tris buffer (pH 8.8) containing 1.0 mM EDTA was carried out. In control experiments, primary antibodies were omitted from the staining procedure, and only Envision$^+$ or Ventana system was applied onto the tissue sections. Counterstaining was performed with hematoxylin.

Acknowledgments

We thank Dr. Nobuyoshi Hiraoka for useful discussion, Dr. Edgar Ong for critical reading of the article, and Ms. Aleli Morse for organizing the article. The work was supported by grants R01 CA33895 (to M.F.) and R01 NS41332 (to Y.Y.) awarded by the National Institutes of Health and by grants-in-aid for Scientific Research from the Ministry of Education, Culture, Sports, Science and Technology of Japan (Priority Area 14082201) and the Ministry of Health, Labor and Welfare of Japan (3rd Term Comprehensive Control Research for Cancer) (to J.N.).

Abbreviations

Endo-*N*, endoneuraminidase-*N*; NCAM, neural cell adhesion molecule; PBS, phosphate-buffered saline; PSA, polysialic

acid; ST8Sia II, α2,8-sialyltransferase II; ST8Sia IV, α2,8-sialyltransferase IV.

References

Angata, K., Nakayama, J., Fredette, B., Chong, K., Ranscht, B., and Fukuda, M. (1997) Human STX polysialyltransferase forms the embryonic form of the neural cell adhesion molecule. Tissue-specific expression, neurite outgrowth, and chromosomal localization in comparison with another polysialyltransferase, PST. *J. Biol. Chem.*, **272**, 7182–7190.

Angata, K., Suzuki, M., and Fukuda, M. (1998) Differential and cooperative polysialylation of the neural cell adhesion molecule by two polysialyltransferases, PST and STX. *J. Biol. Chem.*, **273**, 28524–28532.

Angata, K., Suzuki, M., McAuliffe, J., Ding, Y., Hindsgaul, O., and Fukuda, M. (2000) Differential biosynthesis of polysialic acid on neural cell adhesion molecule (NCAM) and oligosaccharide acceptors by three distinct α 2,8-sialyltransferases, ST8Sia IV (PST), ST8Sia II (STX), and ST8Sia III. *J. Biol. Chem.*, **275**, 18594–18601.

Angata, K., Long, J.M., Bukalo, O., Lee, W., Dityatev, A., Wynshaw-Boris, A., Schachner, M., Fukuda, M., and Marth, J.D. (2004) Sialyltransferase ST8Sia-II assembles a subset of polysialic acid that directs hippocampal axonal targeting and promotes fear behavior. *J. Biol. Chem.*, **279**, 32603–32613.

Chazal, G., Durbec, P., Jankovski, A., Rougon, G., and Cremer, H. (2000) Consequences of neural cell adhesion molecule deficiency on cell migration in the rostral migratory stream of the mouse. *J. Neurosci.*, **20**, 1446–1457.

Chicoine, M.R. and Silbergeld, D.L. (1995) Invading C6 glioma cells maintaining tumorigenicity. *J. Neurosurg.*, **83**, 665–671.

Cosgrove, M., Fitzgibbons, P.L., Sherrod, A., Chandrasoma, P.T., and Martin, S.E. (1989) Intermediate filament expression in astrocytic neoplasms. *Am. J. Surg. Pathol.*, **13**, 141–145.

Cremer, H., Lange, R., Christoph, A., Plomann, M., Vopper, G., Roes, J., Brown, R., Baldwin, S., Kraemer, P., Scheff, S., and others. (1994) Inactivation of the N-CAM gene in mice results in size reduction of the olfactory bulb and deficits in spatial learning. *Nature*, **367**, 455–459.

Daniel, L., Durbec, P., Gautherot, E., Rouvier, E., Rougon, G., and Figarella-Branger, D. (2001) A nude mice model of human rhabdomyosarcoma lung metastases for evaluating the role of polysialic acids in the metastatic process. *Oncogene*, **20**, 997–1004.

Eckhardt, M., Muhlenhoff, M., Bethe, A., Koopman, J., Frosch, M., and Gerardy-Schahn, R. (1995) Molecular characterization of eukaryotic polysialyltransferase-1. *Nature*, **373**, 715–718.

Eckhardt, M., Bukalo, O., Chazal, G., Wang, L., Goridis, C., Schachner, M., Gerardy-Schahn, R., Cremer, H., and Dityatev, A. (2000) Mice deficient in the polysialyltransferase ST8SiaIV/PST-1 allow discrimination of the roles of neural cell adhesion molecule protein and polysialic acid in neural development and synaptic plasticity. *J. Neurosci.*, **20**, 5234–5244.

Edelman, G.M. (1984) Modulation of cell adhesion during induction, histogenesis, and perinatal development of the nervous system. *Annu. Rev. Neurosci.*, **7**, 339–377.

Edvardsen, K., Pedersen, P.H., Bjerkvig, R., Hermann, G.G., Zeuthen, J., Laerum, O.D., Walsh, F.S., and Bock, E. (1994) Transfection of glioma cells with the neural-cell adhesion molecule NCAM: effect on glioma-cell invasion and growth *in vivo*. *Int. J. Cancer*, **58**, 116–122.

Finne, J. (1982) Occurrence of unique polysialosyl carbohydrate units in glycoproteins of developing brain. *J. Biol. Chem.*, **257**, 11966–11970.

Fukuda, M. (1996) Possible roles of tumor-associated carbohydrate antigens. *Cancer Res.*, **56**, 2237–2244.

Hallenbeck, P.C., Vimr, E.R., Yu, F., Bassler, B., and Troy, F.A. (1987) Purification and properties of a bacteriophage-induced endo-*N*-acetylneuraminidase specific for poly-α-2,8-sialosyl carbohydrate units. *J. Biol. Chem.*, **262**, 3553–3561.

Hayama, M., Ota, H., Toki, T., Ishii, K., Honda, T., Momose, M., and Nakata, R. (2002) Cell kinetic study of the endometrium by nonisotopic in situ hybridization for histone H3 messenger RNA and immunohistochemistry for Ki-67 and for estrogen and progesterone receptors. *Anat. Rec.*, **266**, 234–240.

Hildebrandt, H., Becker, C., Murau, M., Gerardy-Schahn, R., and Rahmann, H. (1998a) Heterogeneous expression of the polysialyltransferases ST8Sia II and ST8Sia IV during postnatal rat brain development. *J. Neurochem.*, **71**, 2339–2348.

Hildebrandt, H., Becker, C., Gluer, S., Rosner, H., Gerardy-Schahn, R., and Rahmann, H. (1998b) Polysialic acid on the neural cell adhesion molecule correlates with expression of polysialyltransferases and promotes neuroblastoma cell growth. *Cancer Res.*, **58**, 779–784.

Kaye, A.H., Morstyn, G., Gardner, I., and Pyke, K. (1986) Development of a xenograft glioma model in mouse brain. *Cancer Res.*, **46**, 1367–1373.

Kim, W.J., Terada, N., Nomura, T., Takahashi, R., Lee, S.D., Park, J.H., and Konno, A. (2002) Effect of formaldehyde on the expression of adhesion molecules in nasal microvascular endothelial cells: the role of formaldehyde in the pathogenesis of sick building syndrome. *Clin. Exp. Allergy*, **32**, 287–295.

Kiss, J.Z. and Rougon, G. (1997) Cell biology of polysialic acid. *Curr. Opin. Neurobiol.*, **7**, 640–646.

Kleene, R. and Schachner, M. (2004) Glycans and neural cell interactions. *Nat. Rev. Neurosci.*, **5**, 195–208.

Kleihuses, P. and Cavenee, W.K. (2000) *Pathology and Genetics of Tumors of the Nervous System*. IARC Press, Lyon.

Livingston, B.D. and Paulson, J.C. (1993) Polymerase chain reaction cloning of a developmentally regulated member of the sialyltransferase gene family. *J. Biol. Chem.*, **268**, 11504–11507.

Machida, E., Nakayama, J., Amano, J., and Fukuda, M. (2001) Clinicopathological significance of core 2 β1,6-*N*-acetylglucosaminyltransferase messenger RNA expressed in the pulmonary adenocarcinoma determined by in situ hybridization. *Cancer Res.*, **61**, 2226–2231.

Martersteck, C.M., Kedersha, N.L., Drapp, D.A., Tsui, T.G., and Colley, K.J. (1996) Unique α 2, 8-polysialylated glycoproteins in breast cancer and leukemia cells. *Glycobiology*, **6**, 289–301.

Muller, D., Djebbara-Hannas, Z., Jourdain, P., Vutskits, L., Durbec, P., Rougon, G., and Kiss, J.Z. (2000) Brain-derived neurotrophic factor restores long-term potentiation in polysialic acid-neural cell adhesion molecule-deficient hippocampus. *Proc. Natl. Acad. Sci. U S A.*, **97**, 4315–4320.

Nakayama, J., Fukuda, M.N., Fredette, B., Ranscht, B., and Fukuda, M. (1995) Expression cloning of a human polysialyltransferase that forms the polysialylated neural cell adhesion molecule present in embryonic brain. *Proc. Natl. Acad. Sci. U S A.*, **92**, 7031–7035.

Ohyama, C., Tsuboi, S., and Fukuda, M. (1999) Dual roles of sialyl Lewis X oligosaccharides in tumor metastasis and rejection by natural killer cells. *EMBO J.*, **18**, 1516–1525.

Ong, E., Nakayama, J., Angata, K., Reyes, L., Katsuyama, T., Arai, Y., and Fukuda, M. (1998) Developmental regulation of polysialic acid synthesis in mouse directed by two polysialyltransferases, PST and STX. *Glycobiology*, **8**, 415–424.

Ono, K., Tomasiewicz, H., Magnuson, T., and Rutishauser, U. (1994) N-CAM mutation inhibits tangential neuronal migration and is phenocopied by enzymatic removal of polysialic acid. *Neuron*, **13**, 595–609.

Owens, G.C., Orr, E.A., DeMasters, B.K., Muschel, R.J., Berens, M.E., and Kruse, C.A. (1998) Overexpression of a transmembrane isoform of neural cell adhesion molecule alters the invasiveness of rat CNS-1 glioma. *Cancer Res.*, **58**, 2020–2028.

Perl, A.K., Dahl, U., Wilgenbus, P., Cremer, H., Semb, H., and Christofori, G. (1999) Reduced expression of neural cell adhesion molecule induces metastatic dissemination of pancreatic beta tumor cells. *Nat. Med.*, **5**, 286–291.

Roth, J., Zuber, C., Wagner, P., Taatjes, D.J., Weisgerber, C., and Heitz, P.U. (1988) Reexpression of poly (sialic acid) units of the neural cell adhesion molecule in Wilms tumor. *Proc. Natl. Acad. Sci. U S A.*, **85**, 2999–3003.

Rutishauser, U. and Landmesser, L. (1996) Polysialic acid in the vertebrate nervous system: a promoter of plasticity in cell–cell interactions. *Trends Neurosci.*, **19**, 422–427.

Sabattini, E., Bisgaard, K., Ascani, S., Poggi, S., Piccioli, M., Ceccarelli, C., Pieri, F., Fraternali-Orcioni, G., and Pileri, S.A. (1998) The EnVision++ system: a new immunohistochemical method for diagnostics and research. Critical comparison with the APAAP, ChemMate, CSA, LABC, and SABC techniques. *J. Clin. Pathol.*, **51**, 506–511.

Saffell, J.L., Williams, E.J., Mason, I.J., Walsh, F.S., and Doherty, P. (1997) Expression of a dominant negative FGF receptor inhibits

axonal growth and FGF receptor phosphorylation stimulated by CAMs. *Neuron*, **18**, 231–242.

Scheidegger, E.P., Lackie, P.M., Papay, J., and Rothm, J. (1994) *In vitro* and *in vivo* growth of clonal sublines of human small cell lung carcinoma is modulated by polysialic acid of the neural cell adhesion molecule. *Lab. Invest.*, **70**, 95–106.

Scheidegger, E.P., Sternberg, L.R., Roth, J., and Lowe, J.B. (1995) A human STX cDNA confers polysialic acid expression in mammalian cells. *J. Biol. Chem.*, **270**, 22685–22688.

Seidenfaden, R., Gerardy-Schahn, R., and Hildebrandt, H. (2000) Control of NCAM polysialylation by the differential expression of polysialyltransferases ST8SiaII and ST8SiaIV. *Eur. J. Cell Biol.*, **79**, 680–688.

Seki, T. and Arai, Y. (1991) Expression of highly polysialylated NCAM in the neocortex and piriform cortex of the developing and the adult rat. *Anat. Embryol. (Berl)*, **184**, 395–401.

Smith, S.R., Auerbach, B., and Morgan, L. (1996) Serum neural cell adhesion molecule in multiple myeloma and other plasma cell disorders. *Br. J. Haematol.*, **92**, 67–70.

Suzuki, M., Angata, K., Nakayama, J., and Fukuda, M. (2003) Polysialic acid and mucin type *O*-glycans on the neural cell adhesion molecule differentially regulate myoblast fusion. *J. Biol. Chem.*, **278**, 49459–49468.

Tanaka, F., Otake, Y., Nakagawa, T., Kawano, Y., Miyahara, R., Li, M., Yanagihara, K., Nakayama, J., Fujimoto, I., Ikenaka, K., and Wada, H. (2000) Expression of polysialic acid and STX, a human polysialyltransferase, is correlated with tumor progression in non-small cell lung cancer. *Cancer Res.*, **60**, 3072–3080.

Thorsen, F. and Tysnes, B.B. (1997) Brain tumor cell invasion, anatomical and biological considerations. *Anticancer Res.*, **17**, 4121–4126.

Van Camp, B., Durie, B.G., Spier, C., De Waele, M., Van Riet, I., Vela, E., Frutiger, Y., Richter, L., and Grogan, T.M. (1990) Plasma cells in multiple myeloma express a natural killer cell-associated antigen: CD56 (NKH-1; Leu-19). *Blood*, **76**, 377–382.

Vutskits, L., Djebbara-Hannas, Z., Zhang, H., Paccaud, J.P., Durbec, P., Rougon, G., Muller, D., and Kiss, J.Z. (2001) PSA-NCAM modulates BDNF-dependent survival and differentiation of cortical neurons. *Eur. J. Neurosci.*, **13**, 1391–1402.

Yamaguchi, Y. (2000) Lecticans: organizers of the brain extracellular matrix. *Cell. Mol. Life Sci.*, **57**, 276–289.

Yeh, J.C., Hiraoka, N., Petryniak, B., Nakayama, J., Ellies, L.G., Rabuka, D., Hindsgaul, O., Marth, J.D., Lowe, J.B., and Fukuda, M. (2001) Novel sulfated lymphocyte homing receptors and their control by a Corel extension β 1,3-*N*-acetylglucosaminyltransferase. *Cell*, **105**, 957–969.

Yoshida, Y., Kojima, N., and Tsuji, S. (1995) Molecular cloning and characterization of a third type of *N*-glycan α2,8-sialyltransferase from mouse lung. *J. Biochem. (Tokyo)*, **118**, 658–664.

Zhang, H., Vutskits, L., Calaora, V., Durbec, P., and Kiss, J.Z. (2004) A role for the polysialic acid-neural cell adhesion molecule in PDGF-induced chemotaxis of oligodendrocyte precursor cells. *J. Cell Sci.*, **117**, 93–103.

Transplant International ISSN 0934-0874

ORIGINAL ARTICLE

MCI-186 (edaravone), a free radical scavenger, attenuates hepatic warm ischemia–reperfusion injury in rats

Fumitaka Suzuki,[1,2] Yasuhiko Hashikura,[2] Hirohiko Ise,[1] Akiko Ishida,[3] Jun Nakayama,[3] Masafumi Takahashi,[1] Shin-ichi Miyagawa[2] and Uichi Ikeda[1]

1 Department of Organ Regeneration, Shinshu University Graduate School of Medicine, Asahi, Matsumoto, Japan
2 First Department of Surgery, Shinshu University School of Medicine, Asahi, Matsumoto, Japan
3 Department of Pathology, Shinshu University School of Medicine, Asahi, Matsumoto, Japan

Keywords
chemokine, Kupffer cell, lipid peroxidation, macrophage, neutrophil.

Correspondence
Yasuhiko Hashikura MD, First Department of Surgery, Shinshu University School of Medicine, 3-1-1 Asahi, Matsumoto 390-8621, Japan. Tel.: +81-263-37-2654; fax: +81-263-35-1282; e-mail: yh@hsp.md.shinshu-u.ac.jp

Received: 17 November 2004
Revision requested: 7 December 2004
Accepted: 20 December 2004

doi:10.1111/j.1432-2277.2005.00094.x

Summary

Hepatic warm ischemia–reperfusion injury (IRI) during hepatectomy and liver transplantation is a major cause of liver dysfunction in which the pathologic role of free radicals is a major concern. To assess the effect of MCI-186 (edaravone) on hepatic IRI, male Wistar rats were subjected to partial hepatic ischemia for 60 min after pretreatment with vehicle (group C) or MCI-186 (group M), or after both MCI-186 pretreatment and additional administration of MCI-186 12 h after reperfusion (group MX). Groups M and MX showed significantly lower levels of serum alanine aminotransferase and hepatic lipid peroxidation than group C, and also significantly lower expression levels of mRNA for cytokines, chemokines and intercellular adhesion molecule-1. There were fewer tissue monocytes and neutrophils in groups M and MX than in group C. These effects were more marked in group MX than in group M. Our findings suggest that treatment with MCI-186 attenuates hepatic IRI in this rat *in vivo* model.

Introduction

Warm ischemia–reperfusion injury (IRI) during hepatic resection and liver transplantation may lead to local and systemic organ dysfunction. The local hepatic injury comprises two phases, the acute (early) phase and the subacute (late) phase [1–9]. During the acute phase, Kupffer cells are activated and release oxygen-derived free radicals (ODFRs) and proinflammatory cytokines such as tumor necrosis factor (TNF)-α, interleukin (IL)-1, IL-6 and IL-8. The subacute phase is mediated by infiltrating neutrophils that are primed and activated during the acute phase [1–9]. Chemokines released by Kupffer cells, including CXC chemokines and CC chemokines, may also play important roles in hepatic IRI. CXC chemokines induce neutrophil activation and CC chemokines activate macrophages and T cells and upregulate cell adhesion molecules [10–13]. While recent studies have shown that not only macrophages (Kupffer cells) and neutrophils but also T cells play significant roles in hepatic IRI [3,5,6,14,15], the significance of free radicals in the pathology of the acute and subacute phases of hepatic IRI is thought to be crucial.

MCI-186 [edaravone (3-methyl-1-phenyl-2-pyrazolin-5-one); Mitsubishi Pharma Co., Osaka, Japan] is a free radical scavenger. This reagent has already been applied clinically for the prevention of brain edema in patients with acute cerebral infarction through inhibition of the lipoxygenase pathway in the arachidonic acid cascade and has shown positive results [16–19]. Several reports have described the effects of MCI-186 on hepatic IRI. In *ex vivo* hepatic IRI experiments [20,21], perfusion with Krebs–Henseleit solution cannot reproduce the effects of circulating macrophages and neutrophils, which play major roles in hepatic IRI. In *in vivo* experiments, the efficacy of MCI-186 in attenuating hepatic warm IRI has been evaluated in terms of aspartate aminotransferase, phosphatidylcholine hydroperoxide, adenosine triphosphate [22], and mitochondrial function [23]. However,

the effects of MCI-186 on monocytes, neutrophils and their associated cytokines have not been evaluated.

In the present study, we evaluated the potential of MCI-186 to attenuate hepatic warm IRI in a partial-IRI rat model *in vivo*. We focused on the changes in lipoxygenase activation, monocyte activation, chemokine expression, neutrophil infiltration and hepatic dysfunction resulting from administration of MCI-186.

Materials and methods

Experimental animals and reagents

Male Wistar rats (Clea Japan Inc., Tokyo, Japan) weighing 200–250 g were used. All animals were maintained under standard conditions and fed rodent chow and water *ad libitum*. Twelve hours before surgery, the animals were fasted, but allowed access to water. All experimental procedures were reviewed and approved by the Institutional Animal Care and Use Committee of Shinshu University.

The following monoclonal antibodies were used as primary antibodies for immunohistochemistry: HNEJ-2 (Nikken Seil Co., Shizuoka, Japan) specific for 4-hydroxy-2-nonenal (4-HNE) modified protein, ED-1 (Serotec, Oxford, UK) specific for rat CD163 expressed on free and fixed macrophages, ED-2 (Serotec) specific for rat CD68 expressed on Kupffer cells and on residential macrophages, and HIS48 (BD Biosciences, Palo Alto, CA, USA) specific for rat neutrophils.

Hepatic IRI model

All surgical procedures were carried out according to the protocol described elsewhere [24]. Rats were anesthetized with sodium pentobarbital 50 mg/kg, intraperitoneally (Dainippon Pharmaceutical Co. Ltd, Osaka, Japan). After laparotomy, a microvascular clip (BEAR Medic Co., Chiba, Japan) was used to interrupt the arterial and portal venous supply to the median and left lateral lobes of the liver. This resulted in ischemia of approximately 70% of the whole liver while avoiding portal venous congestion. After 60 min of partial hepatic ischemia, the clamp was removed for reperfusion. The abdomen was closed and 1 ml of saline was administered intravenously. The rats were killed 1, 3, 6 and 24 h after reperfusion, and blood and tissue samples were harvested for analysis.

Experimental protocol

The rats were divided into three groups(Fig. 1). Group S was a sham operation group. Group C comprised IRI model rats, administered saline 5 min before reperfusion. Group M comprised IRI model rats, administered MCI-186 (3 mg/kg) 5 min before reperfusion. Saline and MCI-186 were injected intravenously. The dose and timing of saline and MCI-186 administration were based on previous reports [25–27].

Each group was divided into four subgroups according to the time (h) from reperfusion to killing [groups S-1, S-3, S-6, S-24 ($n = 5$, respectively), C-1 ($n = 6$), C-3 ($n = 5$), C-6 ($n = 7$), C-24 ($n = 7$), M-1 ($n = 6$), M-3 ($n = 5$), M-6 ($n = 7$) and M-24 ($n = 5$)]. For groups S-24, C-24 and M-24, additional administration of saline was performed 12 h after reperfusion.

In addition, considering the short half-life of MCI-186 as well as the acute and subacute mechanisms underlying IRI, a fourth group was additionally administered MCI-186 12 h after reperfusion instead of saline, followed by killing 24 h after reperfusion [group MX-24 ($n = 7$)]. This protocol was used to evaluate the role of MCI-186 in the subacute phase of IRI.

Peripheral blood and tissue samples

Blood samples were obtained via the abdominal aorta. The blood was centrifuged (2500 *g*, 10 min) at room temperature and the plasma was collected and stored at −20 °C until use. Portions of the ischemic and nonischemic lobes were fixed in 10% buffered formalin and embedded in paraffin. Other portions were snap-frozen in

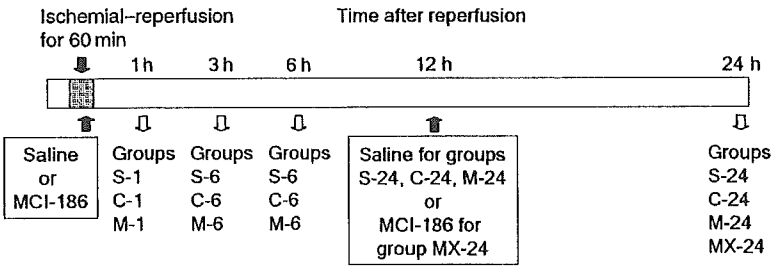

Figure 1 Experimental protocols for rat hepatic ischemia–reperfusion injury models.

liquid nitrogen to extract mRNA and embedded in optimal cutting temperature (OCT) compound (Sakura Finetechnical Co., Tokyo, Japan) for immunohistochemistry, and stored at −80 °C until used.

Measurement of serum aminotransferase

To evaluate hepatic injury, we measured serum alanine aminotransferase (ALT) levels at the time of killing in each group using an AU5232 autoanalyzer (Olympus, Tokyo, Japan), as described previously [24].

Histologic examination

Samples were fixed with 10% buffered formaldehyde and embedded in paraffin. Sections at 3-μm intervals were prepared and stained with hematoxylin and eosin for histologic examination. A blinded analysis was performed by two pathologists to determine the degree of lesions observed ($n = 5$, independent animals in each group). The degrees of sinusoidal congestion, cytoplasmic vacuolization and necrosis of parenchymal cells were evaluated semiquantitatively according to the criteria described in a previous study [28].

Immunohistochemistry

Immunohistochemical detection of lipid peroxidation and inflammatory cell recruitment was carried out. For detection of 4-HNE and macrophages, 10% buffered formaldehyde-fixed and paraffin-embedded tissue samples were cut into 3-μm-thick sections. Antigen retrieval was performed by 25 min of microwave irradiation in 1.0 mM EDTA-Na_2 for 4-HNE, and by 6 min of proteinase K digestion (0.4 mg/ml) for ED-2. No retrieval procedure was performed for ED-1. After antigen retrieval, the sections were incubated with primary antibodies at 4 °C overnight for 4-HNE and at room temperature for 60 min for ED-1 and ED-2. The dilutions of the primary antibodies were 1:80 for 4-HNE, 1:200 for ED-1 and 1:100 for ED-2. Goat anti-mouse immunoglobulin conjugated with peroxidase-labeled dextran polymer (Envision™+ system; Dako, Carpinteria, CA, USA) was used as the secondary antibody.

For detection of neutrophils, we used frozen sections. Samples embedded in OCT compound were cut into 5-μm-thick sections, placed on adhesive-coated slides (Matsunami Glass, Osaka, Japan), and then air-dried. After blocking with 1% normal goat serum in tris-buffered saline, these tissue specimens were incubated at room temperature for 60 min with a primary monoclonal antibody, HIS48. After washing with phosphate-buffered saline, the specimens were incubated using the Envision™+ system.

In a control experiment, the primary antibody was omitted from the staining procedure, and no specific staining was found. Counterstaining was carried out with hematoxylin.

Analysis of mRNA by reverse transcription-polymerase chain reaction (RT-PCR)

Total RNA was extracted from tissue with ISOGEN (Nippon Gene Co. Ltd, Tokyo, Japan). cDNA was reverse-transcribed from 2 μg of total RNA using an Omniscript™ Reverse Transcriptase kit (Qiagen GmbH, Hilden, Germany). The cDNA was amplified by RT-PCR using a *Taq* polymerase core kit (Qiagen GmbH). We prepared primer sets for RT-PCR as shown in Table 1, and the final reaction volume was 25 μl. The samples were loaded into a thermal cycler after determining the optimal number of cycles as follows: 30 cycles of denaturing at 94 °C for 1 min, annealing at 55 °C for 1 min, and extension at 72 °C for 2 min for TNF-α and IL-1β; 30 cycles at 94 °C for 30 s, 58 °C for 1 min, and 72 °C for 1 min for cytokine-induced neutrophil chemoattractant (CINC)-2 and macrophage inflammatory protein (MIP)-2; 25 cycles at 94 °C for 30 s, 60 °C for 1 min, and 72 °C

Table 1. Polymerase chain reaction primer sets for cytokines, chemokines, and adhesion molecule.

	Sense (5′ → 3′)	Anti-sense (5′ → 3′)
β-actin	CGG CAT TGT AAC CAA CAG G	CAT TGC CGA TAG TGA TGA CC
TNF-α	TAC TGA ACT TCG GGG TGA TTG GTC C	CAG CCT TGT CCC TTG AAG AGA A
IL-1β	GCT ACC TAT GTC TTG CCC GT	GAC CAT TGC TGT TTC CTA GG
CINC-2	GCT ACC TAT GTC TTG CCC GT	TGA CCA TCC TTG GAG AGT GGC
MIP-2	AGC TCC TCA ATG CTG TAC TGG	TCT ATC ACA GTG TGG AGG TGG
MCP-1	CTC TTC CTC CAC CAC TAT GC	CTC TGT CAT ACT GGT CAC TTC
MIP-1α	GAA GGA AAG TCT TCT CAG CG	AGA CAT TCA GTT CCA GC
MIP-1β	ATG AAG CTC TGC GTG TCT GC	AGT TCC GAT GAA TCT TCC GG
ICAM-1	GAT GCT GAC CCT CCA CAC CA	CAG GGA CTT CCC ATC CAC CT

TNF-α, tumor necrosis factor alpha; IL-1β, interleukin-1 beta; CINC-2, cytokine-induced neutrophil chemoattractant-2; MIP, macrophage inflammatory protein; MCP, monocyte chemoattractant protein; ICAM-1, intercellular adhesion molecule-1.

for 1 min for monocyte chemoattractant protein (MCP)-1; 30 cycles at 94 °C for 30 s, 56 °C for 1 min, and 72 °C for 1 min for MIP-1α; 30 cycles at 94 °C for 30 s, 60 °C for 1 min, and 72 °C for 1 min for MIP-1β; and 30 cycles at 94 °C for 45 s, 55 °C for 30 s, and 72 °C for 90 s for intercellular adhesion molecule (ICAM)-1. The housekeeping gene β-actin was used as the RT-PCR control, and its cycling program was 25 cycles at 94 °C for 30 s, 60 °C for 1 min, and 72 °C for 1 min. For every gene, the final cycle was followed by soaking for 7 min at 72 °C. RT-PCR products were analyzed using 2.0% agarose gel electrophoresis, and visualized by staining with ethidium bromide.

Statistical analysis

Differences among the groups were evaluated by the Mann–Whitney *U*-test. All values are expressed as mean ± SEM, and data were considered significant at $P < 0.05$.

Results

Serum ALT levels at 1, 3, 6 and 24 h after reperfusion

The serum ALT levels in each group are shown in Fig. 2. Among the groups that underwent ischemia–reperfusion, ALT increased to 11207 ± 1957 U/l in group C-6, but decreased to 3782 ± 1334 U/l in group M-6, which was significantly lower than the level in group C-6. The effect of MCI-186 became less prominent 24 h after reperfusion.

Consequently, we focused on changes occurring 24 h after reperfusion. The ALT levels were 5445 ± 1155 U/l (group C-24) vs. 4405 ± 1387 U/l (group M-24). However, additional administration of MCI-186 at 12 h after reperfusion markedly inhibited the increase in ALT levels to 1065 ± 605 U/l (group MX-24).

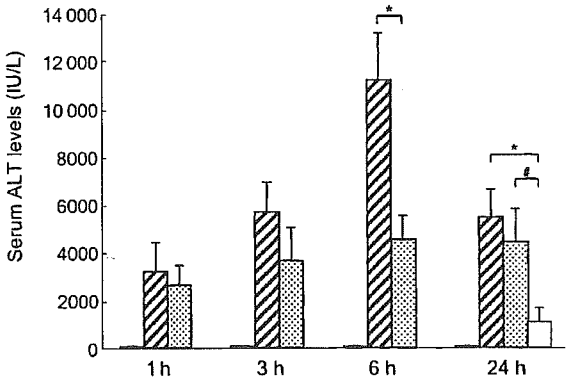

Figure 2 Effects of MCI-186 on serum alanine aminotransferase (ALT) levels. In the acute phase, rats treated with MCI-186 (group M) had lower ALT levels than the saline-treated group (group C). The ALT level in group MX-24 was significantly lower than that in groups C-24 and M-24. Values are expressed as mean ± SEM. *$P < 0.05$ compared with group C; #$P < 0.05$ compared with group M-24. ■, group S; ▨, group C; ▩, group M; □, group MX.

Histologic analysis

No pathologic findings were observed in the liver tissues of the sham control groups (data not shown). In group C-6, liver specimens exhibited focal necrosis, sinusoidal congestion and infiltration of leukocytes, and these changes became more severe in group C-24 (Fig. 3). In contrast, such findings were minimal in group M-6, but were observed in group M-24. In group MX-24, pathologic findings of spotty necrosis, sinusoidal congestion and infiltration of leukocytes were minimal compared with groups C-24 and M-24. These results were confirmed by a semi quantitative assessment, and shown to be significant (Table 2).

Immunohistochemistry for 4-HNE detection

There were no 4-HNE-positive cells in the liver in the sham control groups (data not shown). In groups C-6 and C-24, 4-HNE-positive cells were observed, but the 4-HNE levels were demonstrably reduced in group M-6 (Fig. 4). The number of 4-HNE-positive cells was lower in group MX-24 than in groups C-24 and M-24.

Immunohistochemistry for infiltrating cells

The numbers of cells positive for ED-1 (free macrophages) and ED-2 (resident macrophages) in the ischemic lobes were increased in group C-6, but not in group M-6 (Fig. 5a and b). However, such cells were increased to some extent in group M-24. In group MX-24, the numbers of both ED-1 and ED-2 positive cells were markedly reduced in comparison with groups C-24 and M-24. Figure 5c shows a similar tendency of infiltrated neutrophils into the sinusoids.

Expression of cytokine and chemokine mRNAs

Expression of cytokine and chemokine genes in the ischemic hepatic lobes in groups C and M was compared with that in group S, the sham control group (Fig. 6a). Expression of TNF-α mRNA was high after 1 h (group C-1) and then gradually decreased with time, and was lower in group M-1 than in group C-1 (Fig. 6b). Expression of IL-1 mRNA was high in groups C-1, C-3 and C-6, but attenuated in groups M-3 and M-6. The expression levels of CINC-2 (rat IL-8), MIP-2, MCP-1, MIP-1α and MIP-1β mRNAs were increased in groups C-3 and